

# A novel *NOTCH3* mutation identified in patients with oral cancer by whole exome sequencing

YANJUN YI<sup>1,2</sup>, ZHUOWEI TIAN<sup>2</sup>, HOUYU JU<sup>2</sup>, GUOXIN REN<sup>2</sup> and JINGZHOU HU<sup>2</sup>

<sup>1</sup>Department of Stomatology, Quzhou People's Hospital, Quzhou, Zhejiang 324000; <sup>2</sup>Department of Oral and Maxillofacial-Head and Neck Oncology, Ninth People's Hospital, Shanghai Jiao Tong University School of Medicine, Shanghai Key Laboratory of Stomatology and Shanghai Research Institute of Stomatology, Shanghai 200011, P.R. China

Received February 10, 2016; Accepted April 5, 2017

DOI: 10.3892/ijmm.2017.2965

**Abstract.** Oral cancer is a serious disease caused by environmental factors and/or susceptible genes. In the present study, in order to identify useful genetic biomarkers for cancer prediction and prevention, and for personalized treatment, we detected somatic mutations in 5 pairs of oral cancer tissues and blood samples using whole exome sequencing (WES). Finally, we confirmed a novel nonsense single-nucleotide polymorphism (SNP; chr19:15288426A>C) in the *NOTCH3* gene with sanger sequencing, which resulted in a N1438T mutation in the protein sequence. Using multiple *in silico* analyses, this variant was found to mildly damaging effects on the *NOTCH3* gene, which was supported by the results from analyses using PANTHER, SNAP and SNPs&GO. However, further analysis using Mutation Taster revealed that this SNP had a probability of 0.9997 to be 'disease causing'. In addition, we performed 3D structure simulation analysis and the results suggested that this variant had little effect on the solubility and hydrophobicity of the protein and thus on its function; however, it decreased the stability of the protein by increasing the total energy following minimization (-1,051.39 kcal/mol for the mutant and -1,229.84 kcal/mol for the native) and decreasing one stabilizing residue of the protein. Less stability of the N1438T mutant was also supported by analysis using I-Mutant with a DDG value of -1.67. Overall, the present study identified and confirmed a novel mutation in the *NOTCH3* gene, which may decrease the stability of NOTCH3, and may thus prove to be helpful in cancer prognosis.

## Introduction

Oral cancer, i.e., oral squamous cell carcinoma (OSCC), can affect any part of the oral mucosa and is characterized by sores in the mouth which bleed easily and do not heal. This disease is the sixth most common type of cancer, which affects over 263,000 individuals annually worldwide, and has become a predominant health burden (1,2). The main cause of mortality due to oral cancer is the failure to control the pre-cancerous lesions and lymph node metastasis. Both environmental risk factors, such as betel quid chewing, tobacco use and alcohol consumption, as well as genetic factors are considered of particular importance in the etiology of oral cancer (3). In particular, the combination of these environmental factors and certain genes may increase susceptibility to oral cancer (3). However, these genes have not yet been fully identified.

With the advent of the human genome map involved in different diseases, genetic polymorphisms in certain genes have been found to play crucial roles in driving carcinogenesis. Furthermore, although some biomarkers, such as oral habits are indicators of oral cancer prognostication, genetic variability among different patients should also be taken into consideration. Therefore, genetic polymorphisms have gained colossal importance as novel drug targets or cancer prognostic biomarkers. Furthermore, previous population-based polymorphism studies which detected the association of limited candidate genes or genetic polymorphisms with cancer have not obtained consistent results (4-6). As carcinogenesis is a complex multistep process, it is usually caused by somatic mutations in certain genes. Hence, identifying and assessing polymorphisms in all genes using the method of whole exome sequencing (WES) may be more effective for cancer prognosis and treatment.

WES, a type of massively parallel next-generation sequencing (NGS) technology, is used to effectively identify novel somatic mutations and establish a new genetic basis of certain diseases. It consists of capturing exons, and subsequently high-throughput DNA sequencing. Several small-scale studies have provided some evidence of the potential of WES in identifying disease-driving mutations and genes (2,7,8). For example, using WES within 32 primary oral tumor pairs, Agrawal *et al* found that novel mutations in *FBXW7* and *NOTCH1* may play roles in carcinogenesis of head and neck squamous cell carcinoma (2).

---

**Correspondence to:** Professor Jingzhou Hu, Department of Oral and Maxillofacial-Head and Neck Oncology, Ninth People's Hospital, Shanghai Jiao Tong University School of Medicine, Shanghai Key Laboratory of Stomatology and Shanghai Research Institute of Stomatology, 639 Zhizaoju Road, Shanghai 200011, P.R. China  
E-mail: renzx3@yeah.net

**Key words:** oral cancer, nonsense single-nucleotide polymorphism, whole exome sequencing, NOTCH3

In this study, due to the unreliability of previous clinical markers and the development of NGS, the present study aimed to obtain a landscape of the somatic mutations underlying oral cancer using WES.

## Materials and methods

**Study subjects.** Tumor tissues and blood were collected from treatment-naïve Chinese patients with oral cancer, who then completed the treatment and the follow-up for at least 12 months by their physician. Tumor tissues were obtained by precise laser micro-surgical resection, and blood samples were drawn through the upper arm vein. Ethics approval was obtained from the human Ethics Committee of Ninth People's Hospital (app. no. 2014011). Written informed consent was obtained from all patients. All patients were diagnosed with oral cancer without having any other type of cancer. Histological sections of lesions were examined by two oncopathologists, and the diagnosis was based on the World Health Organization (WHO) guidelines. Clinicopathological staging was determined according to the Union for International Cancer Control (UICC) TNM staging system v6. The patient characteristics are summarized in Table I. All patients received surgery combined with radiation therapy and/or chemotherapy. Each patient was followed-up each month after surgery. The clinical detection of recurrence was confirmed by histopathology. All patients experienced residual or recurrent disease.

**WES.** The bisected tissue samples and blood were stored in liquid nitrogen. Thereafter, genomic DNA was isolated according to standard protocols as previously described (9-11). The genomic DNA libraries were constructed using protocols provided by Illumina (San Diego, CA, USA). Approximately 50 Mb of sequences from the whole exons and their flanking regions were enriched from the fragmented genomic DNA using the Agilent SureSelect DNA Capture array. The captured DNA libraries were processed using the Illumina HiSeq 2500 Genome Analyzer with an overall >10X coverage depth.

**Data processing.** Sequence data in FASTQ files were quality-checked using FASTQC v0.11.4 (<http://www.bioinformatics.babraham.ac.uk/projects/fastqc/>). The filtered sequence reads were mapped to the hg19 reference sequence using Burrows-Wheeler Aligner (BWA) v0.7.12 (<http://sourceforge.net/projects/bio-bwa/>) and SAM files were generated. Local realignment around indels, duplicate removal and Base quality score recalibration were performed using the Genome Analysis Toolkit (GATK) v3.5 (<https://www.broadinstitute.org/gatk/>). Alignment SAM files were converted to BAM files using Samtools v1.3. Somatic variants were called using MuTect v1.1.7 (<https://www.broadinstitute.org/gatk/download/auth?package=MuTect>) with default parameters. High confidence variants were identified with the criteria of a minimum of 10 reads covering a site in the tumor tissue and 8 reads in the blood, and the maximum alternative allele frequency in the blood <0.3 of that in the tumor tissue. Somatic mutations which are defined as called mutations in the absence of corresponding reads in the blood DNA samples were annotated using the Annovar main package ([http://annovar.](http://annovar.openbioinformatics.org/en/latest/)

[openbioinformatics.org/en/latest/](http://annovar.openbioinformatics.org/en/latest/)) to infer the locations of the variants within the genes. Somatic single nucleotide variants (SNVs) were then combined and searched in the dbSNP and COSMIC databases. The reference human genome hg19 and dbSNP132 were used to call and annotate the SNVs. The novel variant identified by WES was verified by Sanger sequencing. The primers used for PCR and sequencing were 5'-AAGTTGTCGTAGAGGCAGGC-3' as the forward primer and 5'-GACCCCTGGCGGCAATG-3' as the reverse primer. PCR was used for Sanger sequencing validation of the new variant. The primers used for PCR and sequencing were forward, 5'-AAGTTGTCGTAGAGGCAGGC-3' and reverse, 5'-GACCCCTGGCGGCAATG-3'. PCR was performed on an ABI9700 PCR instrument (Applied Biosystems, Inc., Foster City, CA, USA). in a 30  $\mu$ l reaction volume including 19 HotStarTaq buffer, 2.8 mM Mg<sup>2+</sup>, 0.1 U of HotStarTaq polymerase (Qiagen, Inc., Valencia, CA, USA), 2 ng of blood genomic DNA, 0.5 pmol of each primer, 0.5 mmol of dNTPs and 0.5 mmol of ddNTPs. Thermocycling was carried out at 94°C for 15 min, followed by 45 cycles at 94°C for 20 sec, 56°C for 30 sec, and 72°C for 1 min, with a final incubation at 72°C for 3 min.

**Evaluation of missense variants.** First of all, the effects of the SNVs were evaluated using Mutation Taster (<http://www.mutationtaster.org/>) (12), which automatically yielded types of predictions, i.e., 'disease\_causing\_automatic', 'disease\_causing', 'polymorphism' and 'polymorphism\_automatic', and the probability P-value of the prediction. A P-value close to 1 indicates a high possibility of the prediction results. A transcript ID and a sequence covering each single-nucleotide polymorphism (SNP) were required as input.

Sorting Intolerant From Tolerant (SIFT; <http://sift.jcvi.org/>) uses a query sequence and multiple alignment information to predict roles of variants (13). The alleles with calculated probabilities <0.05 are predicted to be deleterious; probabilities  $\geq$ 0.05 are tolerated (14). The protein FASTA AA sequence was used as the query sequence and novel mutated SNPs were analyzed.

Polymorphism Phenotyping v2.0 (PolyPhen-2; <http://genetics.bwh.harvard.edu/pph2/>) predicts the influence of variants through automatically selecting 8 sequence-based and 3 structure-based predictive features by an iterative greedy algorithm. If the classifier probability is <0.15, the allele is predicted to be benign, and if the probability is  $\geq$ 0.15, the allele is predicted to be probably or possibly damaging. Protein FASTA AA sequence, amino acid position and amino acid variants are required (15).

PANTHER (<http://www.pantherdb.org/tools/csnpscore-Form.jsp>) predicts the functional consequences of substitutions on the protein by calculating the substitution position-specific evolutionary conservation (subPSEC) score derived from the Hidden Markov Model and alignment score (16). The SNPs with subPSEC  $\leq$  -3 were considered damaging.

SNPs&GO (<http://snps.biofold.org/snps-and-go/>) is based on SVM and functional information codified by gene ontology (GO) terms to predict the impact of protein variations. The present analysis was protein sequence-based. The prediction (either disease or neutral) and RI (probability of disease-related class) are given (17).

Table I. Clinical characteristics of the 5 patients with oral cancer.

Patient ID	Age (years)	Sex	Risk habit <sup>a</sup>	Tumor stage	Tumor stage (TNM)	HPV infection <sup>a</sup>
OC1	44	Male	Alcohol consumption, but no tobacco use	IV	T4a N0	Absent
OC2	44	Male	Alcohol consumption, but no tobacco use	IV	T4a N0	Absent
OC3	46	Male	Alcohol consumption, but no tobacco use	IV	T4a N2b	Absent
OC4	48	Male	Alcohol consumption, but no tobacco use	IV	T4a N0	Absent
OC5	42	Male	Alcohol consumption, but no tobacco use	IV	T4a N2b	Absent

<sup>a</sup>At first presentation.

Table II. Sequencing summary for 5 sample exomes.

Sample (no.)	Tumor tissue (5)	Blood (5)
Reads passed filtration	100021213±7006327	99561798±3048213
Reads mapped (%)	99.86 (99.72-99.91)	99.80 (99.64-99.89)
Capture efficiency (%) <sup>b</sup>	75.12 (69.9-78.2)	74.56 (69-77.8)
Mean depth <sup>a</sup>	139.87±16.29	136.90±11.96
≥1 Coverage (%) <sup>c</sup>	96.78 (96.6-96.9)	96.8 (96.6-97.0)
≥10 Coverage (%) <sup>c</sup>	94.7 (94.3-95.0)	94.66 (94.5-94.8)
≥20 Coverage (%) <sup>c</sup>	92.26 (91.1-93.0)	92.2 (91.7-92.7)
≥40 Coverage (%) <sup>c</sup>	85.86 (82.9-87.9)	85.7 (84.3-87.2)

<sup>a</sup>Data are presented as the means ± SD. <sup>b</sup>Capture efficiency (%), the ratio of the read number that mapped to the exome region to the total read number. <sup>c</sup>Coverage (%), the ratio of the bases number that had been sequenced (≥1, 10, 20 and 40) times to the total base number of the exome region.

SNAP2.0 (<https://roslab.org/services/snap/>) predicts the effect of mutations by identifying all variants based on neutral network method that utilizes protein information. It requires protein sequence as input and yields 80% accuracy (18).

**Modeling protein structures.** I-Mutant v2.0 (<http://folding.biofold.org/i-mutant/i-mutant2.0.html>) is a neural network-based tool for the routine analysis of protein stability and alterations caused by the single-site mutations, which also provides the scores for the Gibbs free energy change (DDG) calculated with the FOLD-X (19). The FOLD-X analysis tool provides the comparison between wild-type and mutant models in the form of van der Waals clashes, which greatly influence the energy decomposition. The protein FASTA AA sequence was used as the query sequence.

The residues mutation was performed using the SwissPDB Viewer viewer and energy minimization for 3D structures was performed by the NOMAD-Ref server ([http://lorenz.immstr.pasteur.fr/gromacs/minimization\\_submission.php](http://lorenz.immstr.pasteur.fr/gromacs/minimization_submission.php)) (20). This server uses Gromacs as the default force field for energy minimization based on the methods of steepest descent, conjugate gradient, and L-BFGS. We used the conjugate gradient method

for optimizing the 3D structures. The deviation between the two structures is evaluated by their root-mean-square deviation (RMSD) values.

To examine the stability of the native and mutant modeled structures, the identification of the stabilizing residues is useful. We used the server SRide (<http://sride.enzim.hu/>) (21) for identifying the stabilizing residues in native protein and mutant models. Stabilizing residues were computed using parameters, such as long-range order, surrounding hydrophobicity, conservation score and stabilization center.

## Results

**Subject characteristics.** In total, tissue and blood samples from 5 patients. All 5 patients were male with a mean age of 44.8±2.28, ranging from 42 to 48 years (Table I). The patients with oral cancer were all HPV-negative and were all alcohol consumers, but were not tobacco users. All patients presented with advanced disease (stage IV)s.

**WES and validation.** Coding exons of approximately 20,000 protein coding genes were sequenced from DNA isolated from the blood and primary tumor of each patient. The mean depths of sequencing were 136.90±11.96 for blood DNA and 139.87±16.29 for tumor DNA. The details for each patient are provided in Table II. The coding regions of genomes of the 5 patients contained 253 somatic variants, of which 51 (20.2%) were predicted to be synonymous, 138 (54.5%) were missense and 5 (2%) nonsense. The average mutation rate/Mb was estimated to be 2.04±0.73 (Table III).

The *TP53* gene was mutated in at least 4 samples and 10 genes in 2 or more samples (Fig. 1). Since NOTCH signaling has been suggested to play important roles in head and neck squamous cell carcinoma (2), a newly identified variant (chr19:15288426A>C) in the *NOTCH3* gene, a homology of *NOTCH1*, and a known variant (chr6:32168732C>T) in the *NOTCH4* gene, another homology of *NOTCH1* attracted our attention. The variant (chr6:32168732C>T) had a frequency of 8.35E-06 in the database of ExAC (<http://exac.broadinstitute.org>) and was a silent mutation, resulting in no amino acid substitution. We then confirmed the newly identified variant (chr19:15288426A>C) in the *NOTCH3* gene using Sanger sequencing (Fig. 2). This nonsense SNP (nsSNP) has the same location with the known nsSNP of rs761506399, but has a different allele mutation. The nsSNP, rs761506399, is an

Table III. Summary of somatic mutation types and prevalence in 5 patients with oral cancer.

Sample	SNV in coding regions				Total	Mutation/Mb DNA	NS/S
	Synonymous	Missense	Stop gained	Others			
OC1	6	13	1	3	23	0.97	2.33
OC2	10	21	0	13	44	1.74	2.10
OC3	10	32	1	14	57	2.21	3.30
OC4	13	41	1	18	73	2.91	3.23
OC5	12	31	2	11	56	2.35	2.75
Total	51	138	5	59	253		

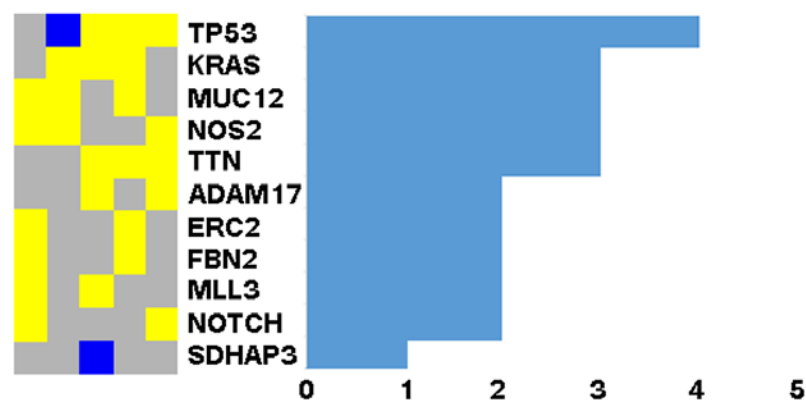


Figure 1. Mutations in genes with two or more cases (left panel), colored by the number of the mutation: blue color, 2; yellow color, 1. The number of cases with mutations in a given gene are shown (right panel). Each column represents a case, and each row represents a gene.

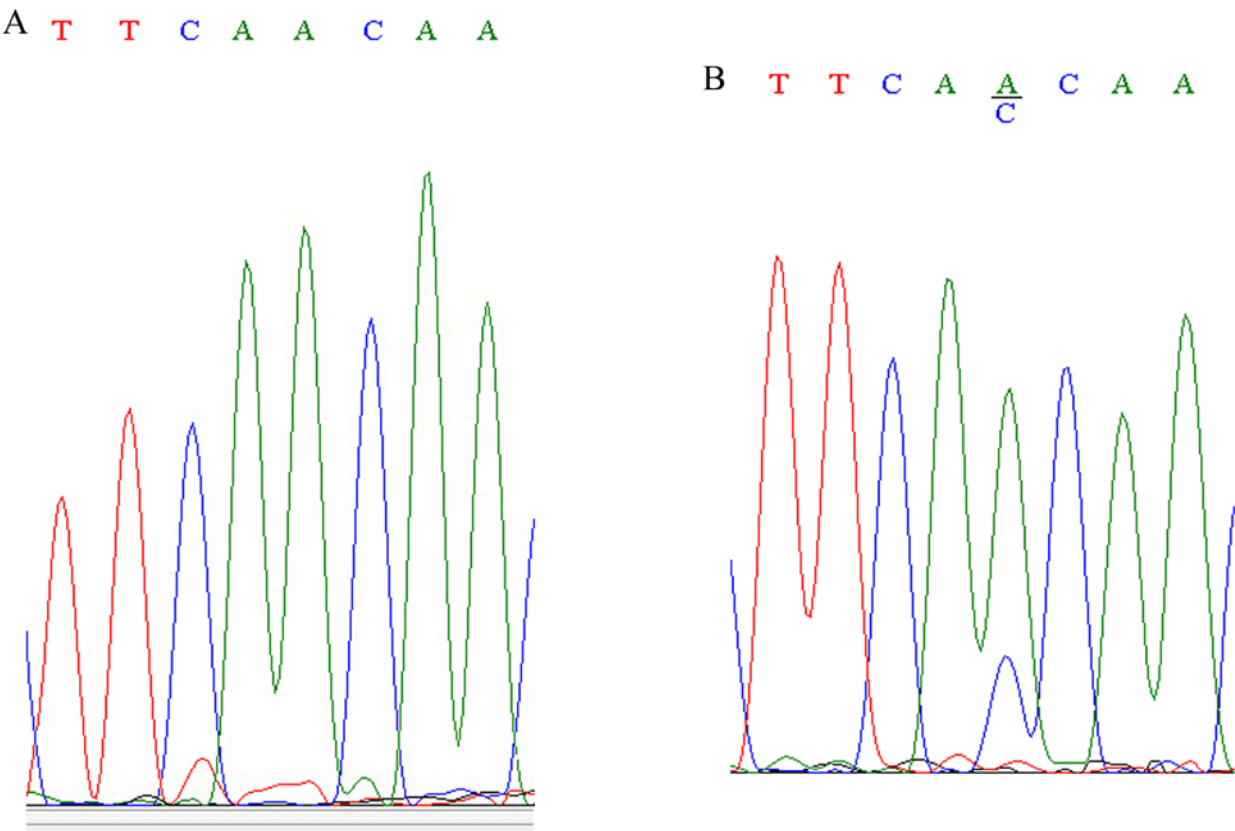


Figure 2. Sequencing electropherograms of the novel NOTCH3 variant at position chr19:15288426A>C, causing an Asn changing into Thr substitution (N1438T). (A) Results from blood sample. (B) Results from tumor tissue.

Table IV. List of results of SIFT, PolyPhen, Panther, SNPs&amp;GO, I-Mutant and SNAP2.

SNP location	AA change	SIFT (score) <sup>a</sup>	PolyPhen (PSIC score)	PANTHER (subPSEC) <sup>b</sup>	SNPs&GO (RI)	I-Mutant (DDG)	SNAP2 (expected accuracy)
chr19:1528842 6T>G	N1438T	Tolerated (0.24)	Probably damaging (0.986)	-2.0575	Neutral (5)	Stability decreases (-1.67)	Effect (85%)

<sup>a</sup>SNPs with scores  $\leq 0.05$  are damaging; <sup>b</sup>SNPs with subPSEC  $\leq -3$  are damaging. SIFT, Sorting Tolerant From Intolerant; PolyPhen, Polymorphism Phenotyping v2.0.

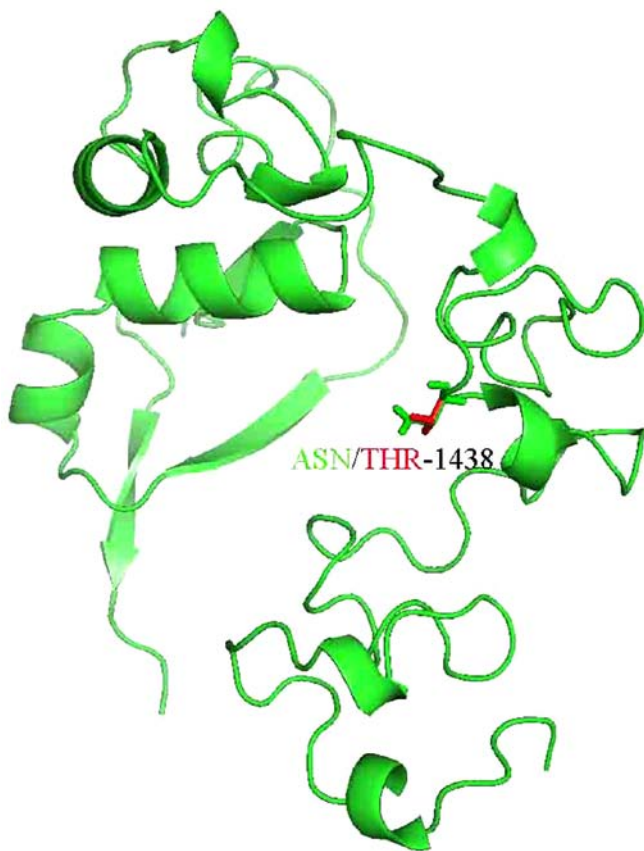


Figure 3. Superimposed structures of native NOTCH3 domain (green) and mutant NOTCH3 domain showing the mutated residue 1438T (red).

A>G mutation and results in 1438 Asn changing into Ser, while the new variant is an A>C mutation and results in 1438 Asn changing into Thr.

**Evaluation of the variant.** We first evaluated the functional effect of this nsSNP by Mutation Taster, which was predicted to be 'disease causing' with a probability of 0.9997 and suggested to possibly affect protein features.

Subsequently, SIFT, which predicts tolerated and deleterious substitutions at each position of the query sequence with multiple alignment score (13), indicated that this nsSNP was tolerated (score, 0.24) (Table IV). PolyPhen-2, which predicts the functional importance of an allele replacement using a training set and naive Bayes classifier, indicated that this nsSNP was 'possibly damaging' with a score of 0.986. We

also examined the probability of the variant causing a deleterious functional change by PANTHER, which is based on the Hidden Markov model and alignment score in a very low value of subPSEC, -2.0575. Another method utilized was SNAP2.0, which is a neutral network method combined with a training set. It designated that this nsSNP affects the function of the NOTCH3 protein. Finally, the mutants were analyzed using SNPs&GO, which is an SVM-based classifier and obtains quite accurate (79%) results. SNPs&GO predicted that this nsSNP was neutral (RI=5) (Table IV).

**3D structure analysis.** I-Mutant v2.0, which is a neural network based tool for the routine analysis of protein stability and alterations caused by the single-site mutations, indicated that it can decrease protein stability with a DDG value of -1.67 (Table IV).

Thus, the 3D structure of NOTCH3 or the domain of NOTCH3 was analyzed. The 3D structure of part of NOTCH3 was resolved as 4ZLP.pdb and the novel mutation was located within the sequence of 4ZLP.pdb. Subsequently, the mutation residues of NOTCH3 were analyzed using the SwissPDB Viewer and energy minimization for 3D structures was performed using the NOMAD-Ref server (20) (Fig. 3). We used the conjugate gradient method for optimizing the 3D structures. The total energy for the native structure was -1,229.84 kcal/mol, and that for the mutant structure (N1438T) was -1,051.39 kcal/mol. The difference between the wild-type structure and the N1438T structure was evaluated by the RMSD value of 1.63.

The computed total solvent accessible surface area of the wild-type protein was 10,287 Å<sup>2</sup> and the surface area excluding the solvent was 8,285 Å<sup>2</sup>, while the total solvent accessible surface area of the N1438T protein was 10,268 Å<sup>2</sup>, and the surface area excluding the solvent was 8,268 Å<sup>2</sup>. The mutant amino acid reduces the solvent accessible surface area by 19 Å<sup>2</sup> for N1438T, and solvent excluded surface area by 17 Å<sup>2</sup> in spite of having more number of atoms as compared to the wild-type. The reduction in surface area may have little effect on the solubility of the protein, and thus on its function. The mutant amino acid is also an AA without charge just like the wide type AA. The hydrophobicity slightly increases for domain with mutant AA (data not shown).

The SRide server (21) was used to identify the stabilizing residues of the native structure and mutant modeled structures with the conservation score threshold of 6, LRO threshold of 0.012, and surrounding hydrophobicity threshold of 20. Four stabilizing residues were identified in the native structure, which were CYS67, ASP70, GLY110 and PRO173. The single-mutant

model (N1438T) has 3 identified stabilizing residues, which were CYS67, ASP70 and GLY110. This analysis revealed that one stabilizing residue in the N1438T-mutant model less than the native protein structure may decrease the stability of the N1438T mutant protein.

## Discussion

Oral cancer has become a serious health concern. It is characterized by a high incidence, low survival rate and severe functional impairment and cosmetic deformity accompanying treatment. Both genetic and environmental factors are widely recognized to result in individual susceptibility to this disease (3). In this study, we identified a novel *NOTCH3* mutation in patients with oral cancer using WES.

Since WES has been proven to be an effective method for a more comprehensive dissection to genomic variation in gene coding regions, it is often used to reveal subtle genetic variations in cancer genomes, to understand the process of tumorigenesis, and fulfill personalized therapies. However, there are some technical limitations to WES. One of these is the identified mutations without underlying a mendelian disorder; the other is the mutant alleles located in the coding regions that are not well covered by WES; the last is the obscured specific copy to which the variant maps due to the presence of pseudogenes or repetitive regions (22). Thus, we only studied somatic variants in the present study and confirmed them with Sanger sequencing.

NOTCH, initially identified in *Drosophila*, is a large transmembrane protein containing epidermal growth factor-like (EGFL) repeats (23,24). There are 4 NOTCH receptors in mammals, i.e., NOTCH 1, 2, 3 and 4, which can bind with NOTCH ligands. They are also transmembrane proteins containing multiple EGFL repeats, including Jagged1, Jagged2, Delta1, Delta3 and Delta4 (25). NOTCH signaling is activated by receptor-ligand interaction during cell-cell contacts, resulting in the proteolytic release of the NOTCH intracellular (NIC) domain into the nucleus and the interaction of NIC with DNA-binding protein to activate transcription of genes involved in a number of cellular properties (25). NOTCH activity affects the implementation of differentiation, proliferation and apoptotic programs to control a broad spectrum of developmental processes, such as neurogenesis, hematopoiesis, vasculogenesis, keratinocyte growth or differentiation (26). Since NOTCH activation can maintain cancer stem cells in some tissues, whereas it can terminate their differentiation in others, NOTCH signaling may play dual roles in cancer, depending on the cellular and tissue context (27), such as an oncogene in non-small cell lung cancer, ovarian carcinoma and osteosarcoma (28-30), whereas it can act as a suppressor gene in chronic myelomonocytic leukemia (CMML) and skin cancer (31,32). As regards the role of NOTCH signaling in oral cancer, both Köse *et al* (33) and Agrawal *et al* (2) found that *NOTCH1* was involved in normal oral mucosa or head and neck squamous cell carcinoma. It has been suggested that NOTCH signaling is functionally activated in OSCC (34). Previous expression array studies have suggested the significant upregulation of NOTCH4 and Jagged1 in OSCC compared to normal oral tissue (35,36). Furthermore, higher expression rates of NOTCH1 and NOTCH3 have been observed in tongue carcinoma compared to adjacent nonneoplastic tissues (37).

These data indicated that the NOTCH signaling pathway may play important roles in the development of oral cancer.

In this study, we reported one variant in the *NOTCH3* and *NOTCH4* gene, respectively. The variant in the *NOTCH4* gene was known with the frequency of 8.35E-06 in database of ExAC. While the variant (chr19:15288426A>C) in the *NOTCH3* gene was novel. Multiple *in silico* analyses were then performed to identify the roles of the variant on the *NOTCH3*.

SIFT is an advantageous analysis tool that can be used to distinguish damaging SNPs with only ~20% false-positive error and ~90% true-positive prediction (13). PolyPhen-2 is a structural modification analysis tool and can achieve true positive prediction rates of 92 and 73% on a training dataset and test dataset at a false-positive rate of 20% (15). Both SIFT and PolyPhen suggested that this variant had mildly damaging effects on the *NOTCH3* gene, which was supported by the results of the analysis using PANTHER, SNAP and SNPs&GO. However, this SNP had a probability of 0.9997 to be 'disease causing', as shown by Mutation Taster analysis. Thus, 3D structure simulation analysis was performed. Our 3D structure models suggested this variant had little effects on the solubility and hydrophobicity of the protein and thus its function, but can decrease the stability of the protein by increasing the total energy following minimization and decreasing the stabilizing residues of the protein. Furthermore, I-Mutant supported that this variant can decrease protein stability with a DDG value of -1.67.

In conclusion, the present study identified a novel variant (chr19:15288426A>C) in the *NOTCH3* gene using WES and confirmed it using Sanger sequencing. With multiple *in silico* analyses and 3D structure simulation, it is suggested that this variant has mildly damaging effects on the function of *NOTCH3* gene, but can decrease protein stability. Thus, this variant may be helpful in cancer prognosis and therapeutic decision-making.

## Acknowledgements

This study was supported by grants from the Project of the National Natural Science Foundation of China (grant nos. 31140007 and 81472516), the Natural Science Foundation of Shanghai (no. 14ZR1424200) and the Shanghai Leading Academic Discipline Project (no. S30206).

## References

1. Haddad RI and Shin DM: Recent advances in head and neck cancer. *N Engl J Med* 359: 1143-1154, 2008.
2. Agrawal N, Frederick MJ, Pickering CR, Bettegowda C, Chang K, Li RJ, Fakhry C, Xie TX, Zhang J, Wang J, *et al*: Exome sequencing of head and neck squamous cell carcinoma reveals inactivating mutations in NOTCH1. *Science* 333: 1154-1157, 2011.
3. Su CW, Huang YW, Chen MK, Su SC, Yang SF and Lin CW: Polymorphisms and plasma levels of tissue inhibitor of metalloproteinase-3: Impact on genetic susceptibility and clinical outcome of oral cancer. *Medicine (Baltimore)* 94: e2092, 2015.
4. Liu H, Jia J, Mao X and Lin Z: Association of CYP1A1 and GSTM1 polymorphisms with oral cancer susceptibility: A Meta-analysis. *Medicine (Baltimore)* 94: e895, 2015.
5. Liu J, Song J, Wang MY, He L, Cai L and Chou KC: Association of EGF rs4444903 and XPD rs13181 polymorphisms with cutaneous melanoma in Caucasians. *Med Chem* 11: 551-559, 2015.
6. Cai L, Huang W and Chou KC: Prostate cancer with variants in CYP17 and UGT2B17 genes: A meta-analysis. *Protein Pept Lett* 19: 62-69, 2012.

7. Li C, Gao Z, Li F, Li X, Sun Y, Wang M, Li D, Wang R, Li F, Fang R, *et al*: Whole exome sequencing identifies frequent somatic mutations in cell-cell adhesion genes in Chinese patients with lung squamous cell carcinoma. *Sci Rep* 5: 14237, 2015.
8. Bell D, Berchuck A, Birrer M, Chien J, Cramer DW, Dao F, Dhir R, DiSaia P, Gabra H, Glenn P, *et al*: Cancer Genome Atlas Research Network: Integrated genomic analyses of ovarian carcinoma. *Nature* 474: 609-615, 2011.
9. Jiang SY, Li LL, Yue J, Chen WZ, Yang C, Wan CL, He L, Cai L and Deng SL: The effects of SP110's associated genes on fresh cavitary pulmonary tuberculosis in Han Chinese population. *Clin Exp Med* 16: 219-225, 2016.
10. Hao CQ, Zhou Y, Wang JP, Peng MJ, Xie YM, Kang WZ, Sun L, Wan CL, He G and He L, *et al*: Role of Nogo-A in the regulation of hepatocellular carcinoma SMMC-7721 cell apoptosis. *Mol Med Rep* 9: 1743-1748, 2014.
11. Cai L, Deng SL, Liang L, Pan H, Zhou J, Wang MY, Yue J, Wan CL, He G and He L, *et al*: Identification of genetic associations of SP110/MYBBP1A/RELA with pulmonary tuberculosis in the Chinese Han population. *Hum Genet* 132: 265-273, 2013.
12. Schwarz JM, Rödelserperger C, Schuelke M and Seelow D: MutationTaster evaluates disease-causing potential of sequence alterations. *Nat Methods* 7: 575-576, 2010.
13. Ng PC and Henikoff S: SIFT: Predicting amino acid changes that affect protein function. *Nucleic Acids Res* 31: 3812-3814, 2003.
14. Ng PC and Henikoff S: Predicting the effects of amino acid substitutions on protein function. *Annu Rev Genomics Hum Genet* 7: 61-80, 2006.
15. Adzhubei IA, Schmidt S, Peshkin L, Ramensky VE, Gerasimova A, Bork P, Kondrashov AS and Sunyaev SR: A method and server for predicting damaging missense mutations. *Nat Methods* 7: 248-249, 2010.
16. Thomas PD, Campbell MJ, Kejariwal A, Mi H, Karlak B, Daverman R, Diemer K, Muruganujan A and Narechania A: PANTHER: A library of protein families and subfamilies indexed by function. *Genome Res* 13: 2129-2141, 2003.
17. Capriotti E, Calabrese R, Fariselli P, Martelli PL, Altman RB and Casadio R: WS-SNPs&GO: A web server for predicting the deleterious effect of human protein variants using functional annotation. *BMC Genomics* 14 (Suppl 3): S6, 2013.
18. Bromberg Y and Rost B: SNAP: Predict effect of non-synonymous polymorphisms on function. *Nucleic Acids Res* 35: 3823-3835, 2007.
19. Capriotti E, Fariselli P and Casadio R: I-Mutant2.0: Predicting stability changes upon mutation from the protein sequence or structure. *Nucleic Acids Res* 33: W306-W310, 2005.
20. Lindahl E, Azuara C, Koehl P and Delarue M: NOMAD-Ref: Visualization, deformation and refinement of macromolecular structures based on all-atom normal mode analysis. *Nucleic Acids Res* 34: W52-W56, 2006.
21. Magyar C, Gromiha MM, Pujadas G, Tusnády GE and Simon I: SRide: A server for identifying stabilizing residues in proteins. *Nucleic Acids Res* 33: W303-W305, 2005.
22. Yang Y, Muzny DM, Reid JG, Bainbridge MN, Willis A, Ward PA, Braxton A, Beuten J, Xia F, Niu Z, *et al*: Clinical whole-exome sequencing for the diagnosis of mendelian disorders. *N Engl J Med* 369: 1502-1511, 2013.
23. Leong KG and Karsan A: Recent insights into the role of Notch signaling in tumorigenesis. *Blood* 107: 2223-2233, 2006.
24. Mohr OL: Character changes caused by mutation of an entire region of a chromosome in *Drosophila*. *Genetics* 4: 275-282, 1919.
25. Callahan R and Egan SE: Notch signaling in mammary development and oncogenesis. *J Mammary Gland Biol Neoplasia* 9: 145-163, 2004.
26. Mitsiadis TA, Lardelli M, Lendahl U and Thesleff I: Expression of Notch 1, 2 and 3 is regulated by epithelial-mesenchymal interactions and retinoic acid in the developing mouse tooth and associated with determination of ameloblast cell fate. *J Cell Biol* 130: 407-418, 1995.
27. Roy M, Pear WS and Aster JC: The multifaceted role of Notch in cancer. *Curr Opin Genet Dev* 17: 52-59, 2007.
28. Jin MM, Ye YZ, Qian ZD and Zhang YB: Notch signaling molecules as prognostic biomarkers for non-small cell lung cancer. *Oncol Lett* 10: 3252-3260, 2015.
29. Park JT, Li M, Nakayama K, Mao TL, Davidson B, Zhang Z, Kurman RJ, Eberhart CG, Shih IeM and Wang TL: Notch3 gene amplification in ovarian cancer. *Cancer Res* 66: 6312-6318, 2006.
30. Engin F, Bertin T, Ma O, Jiang MM, Wang L, Sutton RE, Donehower LA and Lee B: Notch signaling contributes to the pathogenesis of human osteosarcomas. *Hum Mol Genet* 18: 1464-1470, 2009.
31. Klinakis A, Lobry C, Abdel-Wahab O, Oh P, Haeno H, Buonamici S, van De Walle I, Cathelin S, Trimarchi T, Araldi E, *et al*: A novel tumour-suppressor function for the Notch pathway in myeloid leukaemia. *Nature* 473: 230-233, 2011.
32. Nicolas M, Wolfer A, Raj K, Kummer JA, Mill P, van Noort M, Hui CC, Clevers H, Dotto GP and Radtke F: Notch1 functions as a tumor suppressor in mouse skin. *Nat Genet* 33: 416-421, 2003.
33. Köse O, Lalli A, Kutulola AO, Odell EW and Waseem A: Changes in the expression of stem cell markers in oral lichen planus and hyperkeratotic lesions. *J Oral Sci* 49: 133-139, 2007.
34. Hijioka H, Setoguchi T, Miyawaki A, Gao H, Ishida T, Komiya S and Nakamura N: Upregulation of Notch pathway molecules in oral squamous cell carcinoma. *Int J Oncol* 36: 817-822, 2010.
35. Ha PK, Benoit NE, Yochem R, Sciubba J, Zahurak M, Sidransky D, Pevsner J, Westra WH and Califano J: A transcriptional progression model for head and neck cancer. *Clin Cancer Res* 9: 3058-3064, 2003.
36. Leethanakul C, Patel V, Gillespie J, Pallente M, Ensley JF, Koontongkaew S, Liotta LA, Emmert-Buck M and Gutkind JS: Distinct pattern of expression of differentiation and growth-related genes in squamous cell carcinomas of the head and neck revealed by the use of laser capture microdissection and cDNA arrays. *Oncogene* 19: 3220-3224, 2000.
37. Zhang TH, Liu HC, Zhu LJ, Chu M, Liang YJ, Liang LZ and Liao GQ: Activation of Notch signaling in human tongue carcinoma. *J Oral Pathol Med* 40: 37-45, 2011.